Extreme-Quality Computational Imaging via Degradation Framework Supplementary File

Shiqi Chen, Huajun Feng, Keming Gao, Zhihai Xu, Qi Li, Yueting Chen
College of Optical Science and Engineering, Zhejiang University
Hangzhou, Zhejiang, China
{chenshiqi, fenghj, gaokeming, Xuzh, liqi, chenyt}@zju.edu.cn

1. Strehl Ratio *vs.* Receptive Field

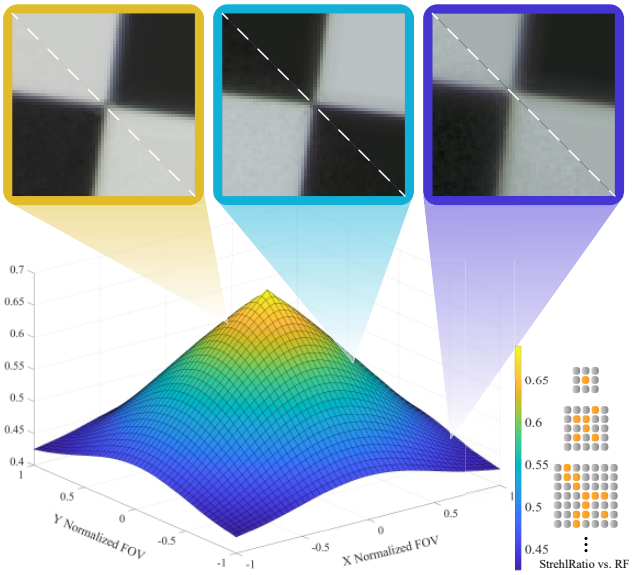

Figure 1. **The relationship between Strehl Ratio and Receptive Field.** The simulation results generated by the degradation framework are compared with the corresponding patch in real photographs.

At the same aperture diameter, the Strehl Ratio indicates the light intensity ratio of the image formed by the actual optical system (with aberration) to the ideal Gaussian image point of the ideal optical system (without aberration). Therefore, the approximate receptive field (RF) of *deep linear network* can be derived by the following equation:

$$RF = \alpha \cdot \frac{l_{airy}}{l_{pixel} \cdot \mathcal{S}(fov)}, \tag{1}$$

Where l_{airy} is the diameter of lenses airy disk, l_{pixel} is the sensor pixel pitch, $\mathcal{S}(fov)$ is the Strehl Ratio *vs.* FOV curve, α is the augmentation coefficient and is set as 1.5 empirically. As shown in Fig. 1, the RF of *deep linear network* will vary with the Strehl Ratio of optical design. And the receptive field of *deep linear network* is increased by concatenating convolution layers in the model. The checkerboards, when supplied with the estimated degradation of different FOVs, are compared with the corresponding real photographs.

2. Authenticity of Degradation Framework

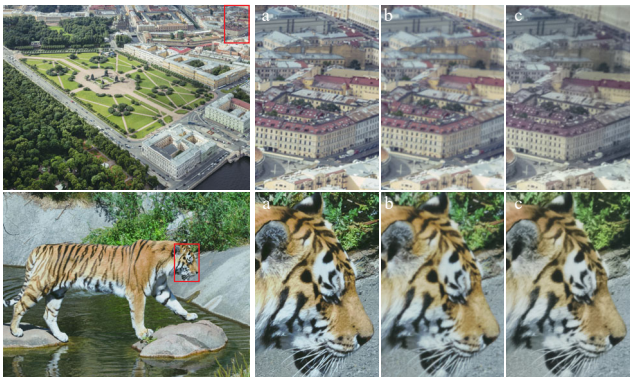

Figure 2. **Comparison of real photographs and simulation results.** (a) is the warpped digital images, (b) is the simulation result of our framework when input (a), and (c) is the real photograph.

To further validate the authenticity of the degradation framework, we print digital images into high-quality posters and photograph them for comparison with the results simulated by our framework. It is worth mentioning that, due to the differences in brightness, tone, and relative position, we perform registration operations on the simulated images to acquire the results that are close to the real photographs. These registration operations will not influence the degradation of a figure, they only change the color and brightness. As shown in Fig. 2, the simulation images generated by the proposed framework closely resemble the real photographs. To demonstrate the effect of simulating image quality mutation, we show different positions, especially the edge, of the

compared images. Although we train the proposed framework in a semi-supervised way on the real checkerboard, the framework still can generalize the estimated degradation to natural images.

3. Advantages over KPN

It's worth mentioning that the kernel size of the compared KPN is 19. **The total parameters number of KPN is 34200k**. While the kernel size of our dilated KPN Block is 5. **The total parameters number of our architecture is 8280k**. So the proposed model has a great advantage in light-weighting, in addition to better results. This is crucial in the application of mobile imaging.

4. Quantitive Assessment on Real-world data

Table 1. **Quantitive assessment on real-world images**

Method	NIQE↓		BRISQUE↓	
SRN	4.6416	(32.5%)	43.74	(28.4%)
DeblurGAN-v2	3.7637	(16.8%)	36.53	(14.2%)
IRCNN	3.7745	(17.0%)	36.31	(13.7%)
GLRA	4.4103	(29.0%)	39.24	(20.2%)
SelfDeblur	4.1852	(25.2%)	38.84	(19.3%)
KPN, $k = 19$	3.2177	(2.7%)	36.04	(13.9%)
LP-KPN	3.6494	(14.2%)	36.09	(13.2%)
HUAWEI ISP	3.7194	(15.8%)	31.33	(0.0%)
Ours	3.1310	(0.0%)	33.46	(6.4%)

We perform a quantitive evaluation on the blur resolved real-world image. The assessing indicator includes NIQE and BRISQUE. In addition to the methods used in the main body, we also added the quantitative evaluation of Huawei ISP for comparison. The real-world images to be tested consist of 30 images taken by the HUAWEI HONOR 20. The evaluation are listed in the Table 1.

We also conduct a user study for absolutely subjective evaluation. We collect 20 users for this experiment. After showing three contrast images (KPN, HUAWEI ISP, and Ours) and their small pieces, we asked them to score 1 to 5 from three aspects: resolution, color and overall. The user study is shown in Fig. 3. This result and the quantitive evaluation show that our method outperforms other methods and HUAWEI ISP in many cases. We note that the proposed approach is not as good as HUAWEI ISP in color evaluation. This is because the additional tone mapping gives images a more suitable color for human eye.

5. Ablation Study on Optical Priors

To further validate the effects of the proposed optical priors, we perform a detailed ablation study on each part of our proposal. We use MTFA (the area enclosed by the MTF curve and the axis) and SSIM to evaluate the accuracy of estimation. Because the values of the two indicators are not uniform, we calculate the relative accuracy (value divided by the maximum) for display. The results shows that the pixel-to-pixel supervised loss and the sum2one loss are crucial to help the degradation frameworks make precise estimation. Other priors have positive effects but not obvious.

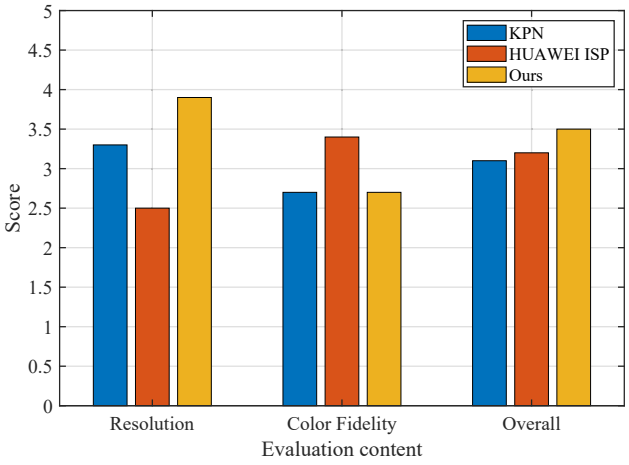

Figure 3. **User study experiments.** We compare three post-processing methods: KPN ($k = 19$), HUAWEI ISP, and Ours. The users are asked to score from: resolution, color, and overall performance. This histogram shows the average score of 20 users.

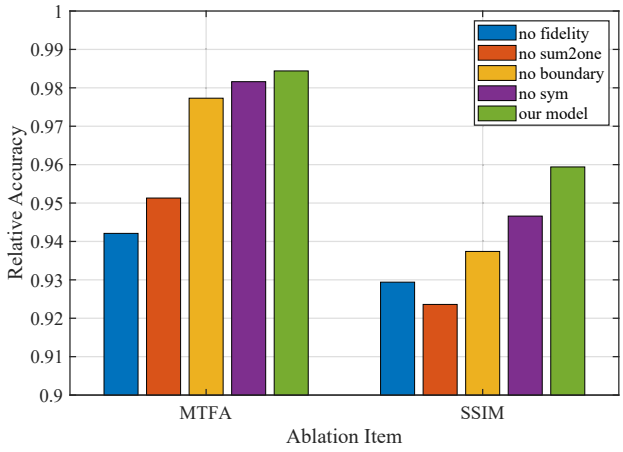

Figure 4. **Optical priors ablation study.** We calculate MTFA and SSIM metrics for evaluation. Relative accuracy is shown because the values of the indicators (MTFA and SSIM) are not uniform. All this results are tested on synthetic data, and the experimental conditions are the same as those in Section 5.1 of the paper.

6. Postprocessing Pipeline *vs.* Commercial ISP

As shown in Fig. 5, the results of the proposed postprocessing pipeline overwhelm the images of HUAWEI ISP.

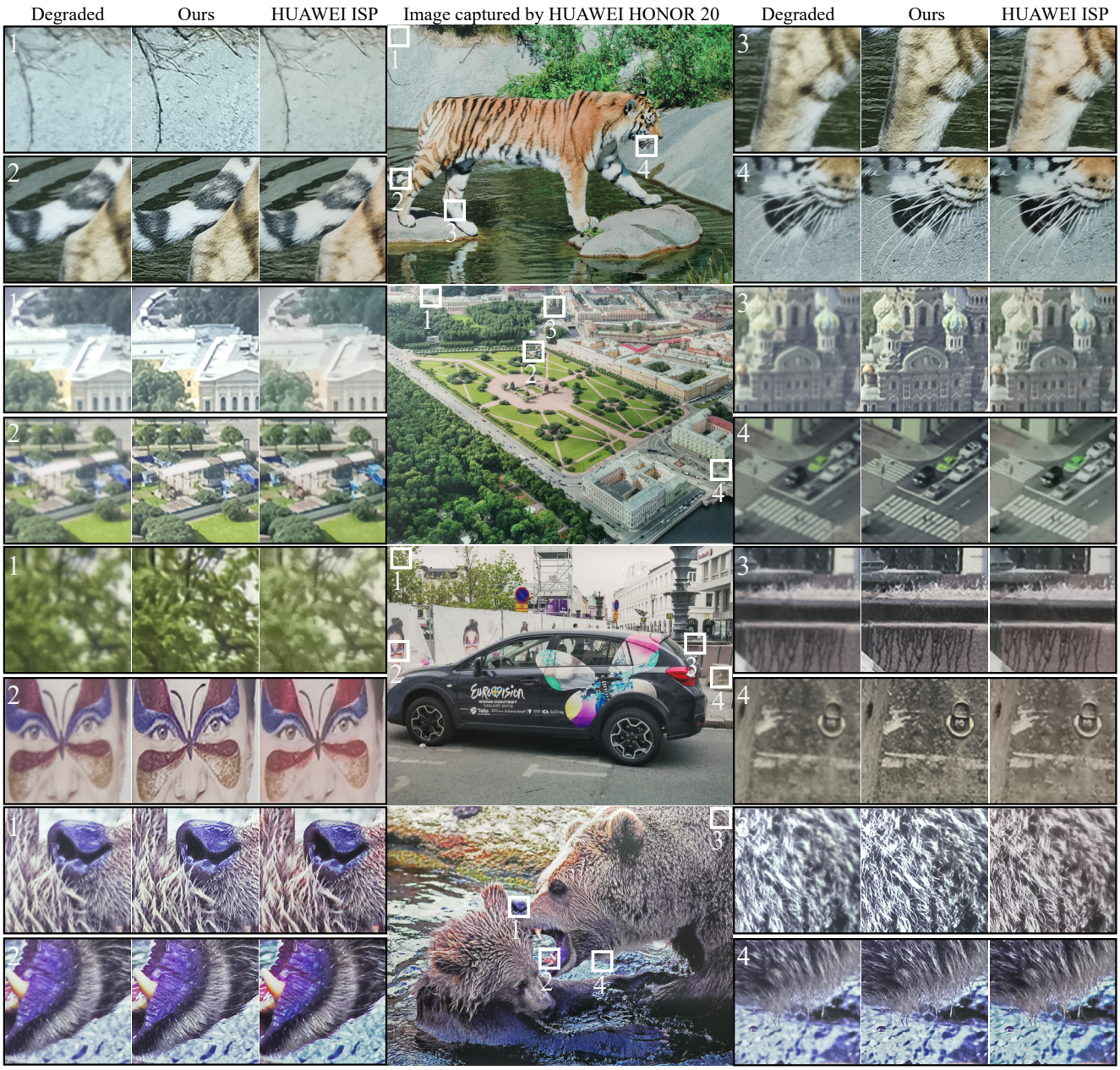

Figure 5. **Postprocessing pipeline *vs.* Commercial ISP.**

For severe degradation in the edge of images, our network performs spatial-adaptive recovery and realizes better visual quality without introducing false texture. Due to the additional toning operation, the results of HUAWEI ISP are somewhat different in color from ours. But this does not affect the evaluation of blur. The time spent on a 3000×4000 image of the proposed network is 0.3 second on average when test on an NVIDIA GeForce GTX 1080Ti. Therefore, the proposed method has a wide range of applications in real-time photography. To prove that our method is still effective on other mobile imaging devices, we re-conducted the above experiments on a customized DSLR camera. We designed the optical lens of this system and its unit uses Canon 80D. The experimental results are shown in Fig. 6, which show that our method is easy to transplant to new imaging devices and can achieve better imaging results than the built-in ISP. **We provide the source code of the proposed Degradation Framework and the FOV-KPN. For more details about our technique, we refer readers to the provided code information.**

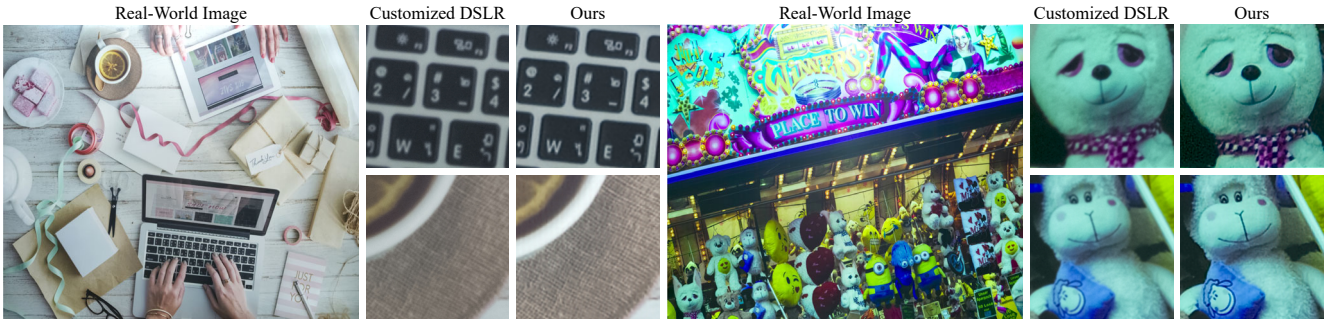

Figure 6. **Postprocessing pipeline *vs.* DSLR ISP.**